A prokaryotic glutamate receptor: homology modelling and molecular dynamics simulations of GluR0

Yalini Arinaminpathy, Philip C. Biggin, Indira H. Shrivastava[1], Mark S.P. Sansom*

Laboratory of Molecular Biophysics, Department of Biochemistry, The University of Oxford, The Rex Richards Building, South Parks Road, Oxford OX1 3QU, UK

Received 16 June 2003; revised 11 September 2003; accepted 12 September 2003

First published online 24 September 2003

Edited by Maurice Montal

Abstract GluR0 is a prokaryotic homologue of mammalian glutamate receptors that forms glutamate-activated, potassium-selective ion channels. The topology of its transmembrane (TM) domain is similar to that of simple potassium channels such as KcsA. Two plausible alignments of the sequence of the TM domain of GluR0 with KcsA are possible, differing in the region of the P helix. We have constructed homology models based on both alignments and evaluated them using 6 ns duration molecular dynamics simulations in a membrane-mimetic environment. One model, in which an insertion in GluR0 relative to KcsA is located in the loop between the M1 and P helices, is preferred on the basis of lower structural drift and maintenance of the P helix conformation during simulation. This model also exhibits inter-subunit salt bridges that help to stabilise the TM domain tetramer. During the simulation, concerted K^+ ion–water movement along the selectivity filter is observed, as is the case in simulations of KcsA. K^+ ion exit from the central cavity is associated with opening of the hydrophobic gate formed by the C-termini of the M2 helices. In the intact receptor the opening of this gate will be controlled by interactions with the extramembranous ligand-binding domains.

Key words: Ion channel; Receptor; Molecular model; MD simulation; Membrane protein

1. Introduction

Ion channels are integral membrane proteins that form specific ion conduction pathways across cell membranes [1]. Channels may be gated by a variety of factors, including changes in transmembrane voltage and binding of ligands to receptor domains. Amongst the ligand-gated ion channels, ionotropic glutamate receptors (iGluRs) mediate excitatory neurotransmission in the central nervous system of mammals. Studies of the pharmacological and physiological properties of neuronal glutamate receptors [2] have shown that iGluRs can be divided into three subtypes based on their sensitivity to the agonists (*RS*)-2-amino-3-(3-hydroxy-5-methylisoxazol-4-yl) propionic acid (AMPA), kainate or *N*-methyl-D-aspartate. All three types of channels are also activated by glutamate, the physiological neurotransmitter. The structure of the extracellular, ligand-binding domain of rat GluR2 has been studied in some depth by X-ray crystallography [3–10], nuclear magnetic resonance [11] and simulation [12,13]. However, the structure of the transmembrane (TM) pore-forming domain remains more elusive.

As for other families of mammalian membrane proteins (e.g. K channel, ABC transporters, aquaporins) bacterial homologues of mammalian glutamate receptors exist [14]. In particular, GluR0 from *Synechocystis* has been shown to have a sequence homologous to mammalian GluRs and to form glutamate-activated ion channels when expressed in *Xenopus* oocytes or HEK cells [15]. The crystal structure of the extracellular ligand-binding domain of GluR0 has been shown to be similar (core Cα root mean square deviation (RMSD) = 0.13 nm in the glutamate-bound forms [16]) to that of the rat GluR2 [16]. Thus, GluR0 provides a model of the (somewhat more complex) mammalian GluRs.

KcsA is a bacterial K^+ channel, the structure of which has been determined in a closed state by X-ray diffraction [17,18]. K^+ channels are tetrameric, with the four subunits surrounding a central pore. Each subunit consists of two TM helices (M1 and M2) plus a pore-forming loop (P). Sequence comparisons suggest a significant homology between the TM domains of KcsA and of GluR0 [15] (within the P region and M2 segments, GluR0 has 44% sequence identity to KcsA) and by extension between K channels and mammalian GluRs [19,14]. Furthermore, the channels formed upon expression of GluR0 are K^+-selective [15]. It is therefore not unreasonable to assume that GluR0 and KcsA share a similar TM fold, although that of GluR0 is inverted in the membrane relative to that of KcsA (Fig. 1A). Studies on AMPA receptors probing accessibility of substituted cysteines to chemical modification [20] are consistent with a KcsA-like fold in these mammalian GluRs, as are scanning mutagenesis studies of GluR6 [21].

Homology modelling and subsequent molecular dynamics (MD) simulations can be used to explore possible models of ion channel TM domains [22]. For example, such methods have been used with some degree of success to explore models of inward rectifier potassium (Kir) channels [23–25] based on the structure of KcsA, even though the sequence identity between Kir channels and KcsA is rather low [26]. In this paper, we present a homology model of the TM domain of GluR0, and explore the structural dynamics of this model in a multi-nanosecond MD simulation in a bilayer-like environment. The results of these studies suggest that the GluR0 TM do-

*Corresponding author. Fax: (44)-1865-275182.
E-mail address: mark.sansom@biop.ox.ac.uk (M.S.P. Sansom).

[1] Present address: National Institute of Health, LECB, NCI, 12B, South Drive, Bethesda, MD 20892, USA.

0014-5793/03/$22.00 © 2003 Published by Elsevier B.V. on behalf of the Federation of European Biochemical Societies.
doi:10.1016/S0014-5793(03)01036-6

main model is stable in such simulations, but that it adopts a closed channel conformation (since it is modelled on KcsA).

2. Materials and methods

The GluR0 sequence was taken from NP_441171 (NCBI Reference Sequence Project accession number). Sequence alignments were performed using Jalview (http://www.ebi.ac.uk:80/jalview/index.html) and ClustalW. The TM helices were predicted using a consensus of the results from the programs DAS (http://www.sbc.su.se/~miklos/DAS/), TMAP (http://www.mbb.ki.se/tmap/), TMHMM (http://cbs.dtu.dk/services/TMHMM-1.0/), TMPred (http://www.ch.embnet.org/software/TMPRED_form.html) and PHDhtm (http://www.embl-heidelberg.de/predictprotein/).

Modeller6 [27,28] was employed to homology model GluR0, using the KcsA crystal structure (1K4C) as the template. Four-fold rotational symmetry was imposed during the modelling procedure. Secondary structure restraints were applied to ensure the M1, P and M2 regions were α-helical. Twenty-five models were generated and these were ranked by analysis of their stereochemistry using Modeller and Procheck [29]. In addition, each model was scored on its deviation from the KcsA structure. From the ensemble, the highest-ranking structure on the basis of these two criteria was selected for further analysis and as a starting structure for MD simulations. The charge states of the ionisable residues in the model were assigned as described in [23,30] using UHBD [31] to estimate electrostatic interactions and solvation energies.

In preparation for simulations, three K^+ ions and water molecules were positioned in binding sites corresponding to the sites found in the X-ray structure of KcsA [18]. Thus, two K^+ ions (K1 and K2) were placed in the filter (at sites S1 and S3 – see Fig. 2) and one (K3) in the central cavity lined by the M2 helices. In addition, eight or nine water molecules were added in the cavity surrounding K3. The resulting model was inserted into a bilayer-mimetic octane slab of thickness ~3.5 nm (Fig. 2) and the system then solvated with SPC [32] water molecules. Cl^- counterions were added at random positions in the bulk solvent region to give overall electrical neutrality. This yielded a system of ~29 800 atoms. Each system was then equilibrated for 0.6 ns by an MD run during which the protein atoms were harmonically restrained. The protein restraints were then removed and production runs of 6 ns duration performed.

MD simulations were run using GROMACS 2.0 [33] (http://rugmd0.chem.rug.nl/gmx/). An electrostatic twin-range cutoff of 1.8/1.4 nm was employed. The van der Waals cut-off was 1.4 nm. The time step for integration was 2 fs, using the LINCS algorithm to constrain bond lengths [34]. Pressure and temperature were controlled using the weak coupling method [35]. Water (and counterions), octane, protein and K^+ were each coupled separately to a temperature bath at 300 K. The pressure in the z direction was maintained close to 1.0 bar using time constant $\tau_p = 1.0$ ps and compressibility $\kappa_z = 4.6 \times 10^{-5}$ bar^{-1}. The x and y dimensions of the simulation box were fixed. Atomic co-ordinates and velocities were saved every 5 ps, and were kept for subsequent analysis using the GROMACS suite of packages.

Structural diagrams were prepared using Molscript [36] and Raster3D [37]. Secondary structure was analysed using DSSP [38].

3. Results and discussion

Two plausible alignments for GluR0 v. KcsA could be obtained (Fig. 1B). Alignment A resembles that of Chen et al. [15]. Note that this places an insertion in the GluR0 region corresponding to the P helix of KcsA. In alignment B, the insertion is located in the loop between the M1 and P helices. The alignments for M1 and M2 are the same for both models. The selectivity filter region is completely conserved between KcsA and GluR0. However, in other regions the sequence conservation is somewhat less. Thus, comparing the M2 helices of KcsA and GluR0, there is ~38% sequence identity and furthermore the glycine (G99 of KcsA) that is conserved amongst K channels and is suggested to form a gating hinge

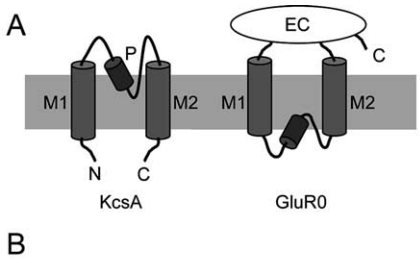

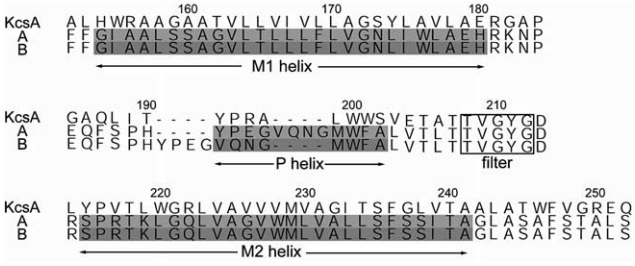

Fig. 1. A: Diagram of KcsA v. GluR0 TM topologies. B: KcsA v. GluR0 sequences, showing the two possible GluR0 alignments. The extents of the M1, P and M2 helices and of the filter region in KcsA are indicated. The numbers at the top correspond to the sequence of GluR0.

[39,40] is *not* conserved in M2 of GluR0. Furthermore, there is only ~12% sequence identity between the P helices of GluR0 and KcsA, and the tryptophan (W68) of the P helix of KcsA that forms a stabilising H-bond to the tyrosine side chain of the selectivity filter (motif GYG) is replaced by a phenylalanine in GluR0, thus removing this potential filter-stabilising element from the GluR0 fold.

Two models were generated, one based on each alignment (denoted model A and B, based on alignment A and B respectively). These were very similar (Cα RMSD = 0.014 nm). As expected the major difference lies in the M1/P loop and P helix region. In model A the P helix is somewhat distorted as a result of the insertion of the four residues YPEG found in GluR0 into the helix. As can be seen from Fig. 3 this results in a longer P helix in model A as compared with a longer M1/P loop in model B. Both of these models were then inserted in a membrane-mimetic octane slab for subsequent simulation studies. Following the pK_A calculations, for both models the majority of all ionisable side chains were found to remain in their default states, yielding a net protein charge of +5 (model A) or +4 (model B).

It has been noted that amphipathic aromatic residues (tryptophan and tyrosine) on the surface of membrane proteins tend to be located in two bands that correspond to the locations of the two lipid headgroup–water interfaces of the bilayer in which the protein is embedded [41]. The outer surfaces of the GluR0 models were examined in terms of the distribution of such residues in relation to obtaining a correct docking of the models into a membrane-mimetic octane slab (Fig. 2A). Rings of Trp and Tyr residues (residues 176, 191, 200 and 228) clearly define the presumed intracellular interface in both GluR0 models. We have also examined the locations of basic (lysine and arginine) side chains that have been suggested to possess a tendency to 'snorkel' to the interface. In both GluR0 models these residues (181, 182, 214, 217 and

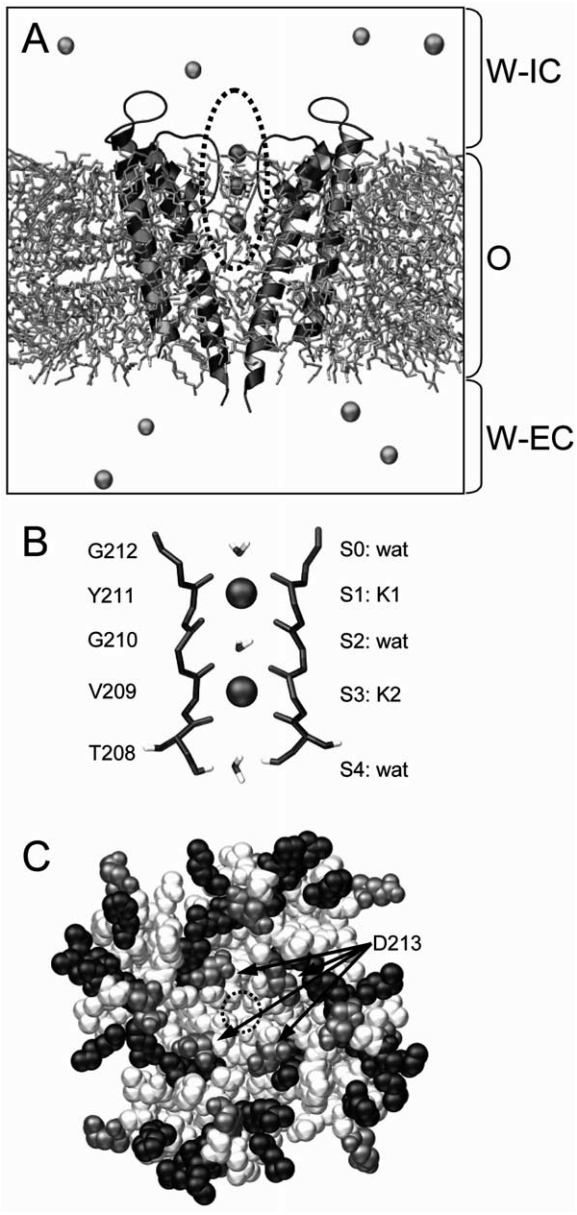

Fig. 2. A: GluR0 TM domain model (model B) embedded in a membrane-mimetic octane slab. K^+ ions and Cl^- counterions are shown. The dotted line ellipse indicates the selectivity filter. B: Filter region (with K^+ ions and water molecules). C: Extracellular entrance to the pore, showing acidic side chains (mid-grey) v. basic side chains (dark grey). The ring of D213 side chains surrounding the pore mouth (dotted circle) is indicated by arrows.

219) are also clustered near the intracellular membrane-solvent interface. Thus the homology models of the GluR0 TM domain are plausible as membrane proteins on the basis of their TM surface side chain distributions.

The filter region (Fig. 2B) of the GluR0 models strongly resembles that of KcsA, as one would expect. Thus, there are five binding sites in the filter from S0 (formed by the G212 carbonyl oxygens) to S4 (formed by the carbonyl oxygens and side chain hydroxyls of T208). The simulations started for a configuration in which K^+ ions were placed in sites S1 and S3, with waters at S0, S2 and S4 (as in previous simulation studies of KcsA [42,43]).

It is also useful to compare the distribution of charged residues in the models and KcsA (Fig. 2C). In KcsA, there is a ring of acidic side chains (D80 in KcsA; aligned with D213 in GluR0 – see Fig. 1B) at the extracellular mouth of the pore. This is also observed in GluR0, where a similar ring of aspartates (D213) is positioned at the corresponding (intracellular) mouth. In addition, the distribution of basic residues at the mouth close to the filter of the channel shows a similarity between GluR0 and KcsA.

Two simulations were set up, one each for model A and model B (Fig. 2). Each system was simulated for 6 ns. The aim of conducting two parallel simulations was to see whether they would enable us to distinguish between the two possible models upon the basis of conformational stability during the simulation.

The conformational stability of the GluR0 models was measured as the global drift from the initial protein conformation via calculation of the RMSD of each model from its initial co-ordinates, evaluated as a function of time (Fig. 4A). Comparison of the Cα RMSDs revealed a small difference between models A and B. In each case there was an initial steep rise in RMSD over the first ~0.1 ns due to model 'relaxation' in the octane/water environment. For model A this was followed by a steady increase in RMSD from ~0.3 nm at 1 ns to ~0.37 nm at 6 ns. In contrast, for model B, the RMSD over the same period oscillates ~0.32 nm rather than rising monotonically. The RMSD of 0.32 nm for model B may be compared with an RMSD of ~0.3 nm for a comparable simulation of KcsA in octane over a similar simulation period [40]. Thus, the overall conformational stability of model B of the GluR0 TM domain in the octane slab environment is similar to that of the 2 Å resolution crystal structure of KcsA. Over a similar period of simulation time the RMSD of KcsA in a POPC bilayer is ~0.15 nm [44]. Clearly the more fluid environment provided by the octane slab allows for greater conformational drift on a ~5 ns timescale.

A clearer distinction between the two models in favour of model B can be made on the basis of the RMSDs of the P helix. Thus the plateau values of the Cα RMSDs of the P helix are ~0.24 nm for model A and ~0.15 nm for model B. We have also calculated the RMSD from an ideal α-helix as a function of time for the P helices in each model (Fig. 4B). The P helices in model B are significantly more stable. In the

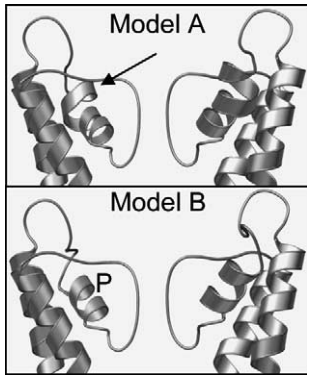

Fig. 3. Comparison of the P helix and filter regions in (A) model A and (B) model B of the GluR0 pore domain. The longer, and distorted, P helix in model A is indicated by an arrow. For each model, only two of the four subunits are shown.

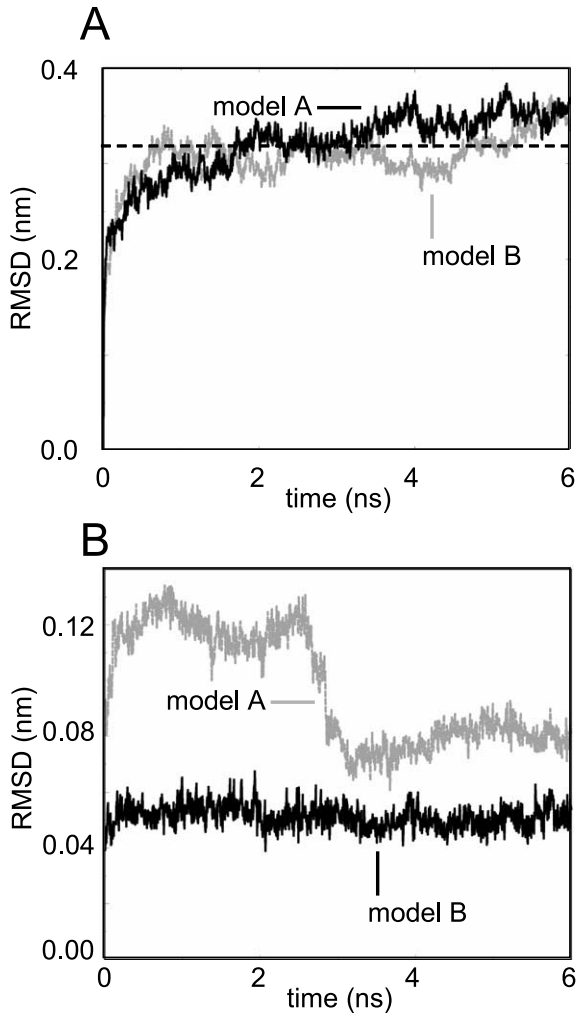

Fig. 4. A: Structural drift shown as RMSDs of all Cαs (black = model A; grey = model B). The horizontal broken line shows the plateau RMSD value for model B. B: P helix deviation from an ideal α-helix backbone vs. time (black = model A; grey = model B).

case of model A, a significant shift in P helix conformation occurs midway through the simulation.

A similar distinction emerges if one compares the secondary structures of the two models over the course of the simulations (data not shown). For both models, the M1 and M2 helices retain their secondary structure content for nearly 100% of the simulation. This is also true of the P helices in model B whereas for model A there is significant loss of secondary structure content in the N-terminal part of the P helix (for residues 187–197). This analysis therefore confirms the greater stability of model B in the region of the P helix. The remainder of the analysis in this paper therefore concerns model B.

A further difference was seen between the two models. In model B, but not in model A, a salt bridge was seen between the side chains of D213 in one subunit and R217 in an adjacent subunit (Fig. 5A). This salt bridge is not present in the initial model but forms at two or three out of the four inter-subunit interfaces after ~2 ns of simulation (Fig. 5B). It may thus be expected to help stabilise the tetramer. This salt bridge is comparable to the D80–R89 inter-subunit salt bridge formed in KcsA, an interaction thought to be conserved in a number of K^+ channels. Mutation of the D80 and/or R89 (or equivalents) results in loss of expression in KcsA [45] and in K_v channels [46,47].

It is important to assess the structural stability of the selectivity filter as it is a key structural element and the basis of observed selectivity for K^+ ions of GluR0 channels [15]. The selectivity filter is formed by the backbone carbonyl groups of the residues Thr^{208}-Val^{209}-Gly^{210}-Tyr^{211}-Gly^{212} which define five potential K^+-binding sites, S0–S4, as in KcsA (Fig. 2B). Visualisation of the filter over the course of the simulation (Fig. 6A) suggests that the K^+ ions help to maintain the conformation of the filter. Thus at the start of the simulation K^+ ions are present in sites S2 and S4, and the filter conformation remains close to that in the (high K^+ concentration) crystal structure. Later on in the simulation K^+ ions leave the filter causing it to distort such that site S4 remains intact but the filter 'closes' in the vicinity of site S2. Distortions of the filter so as to induce a local closed conformation have been observed in crystals of KcsA grown in the presence of a low K^+ concentration [18], and in simulations of mutants of

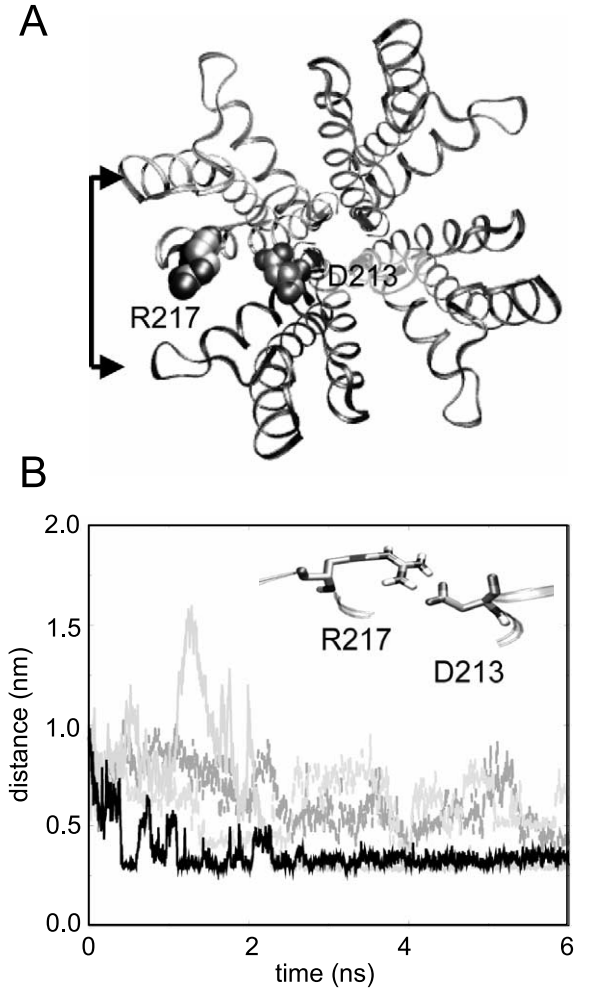

Fig. 5. Inter-subunit salt bridges. A: Ribbon diagram of model B, illustrating the D231/R217 interaction. The view is down the pore axis from the intracellular mouth. B: The distances from the carboxylate oxygen of D213 of one subunit to the guanidinium nitrogen of R217 of an adjacent subunit (see inset figure) are plotted as a function of time for model B.

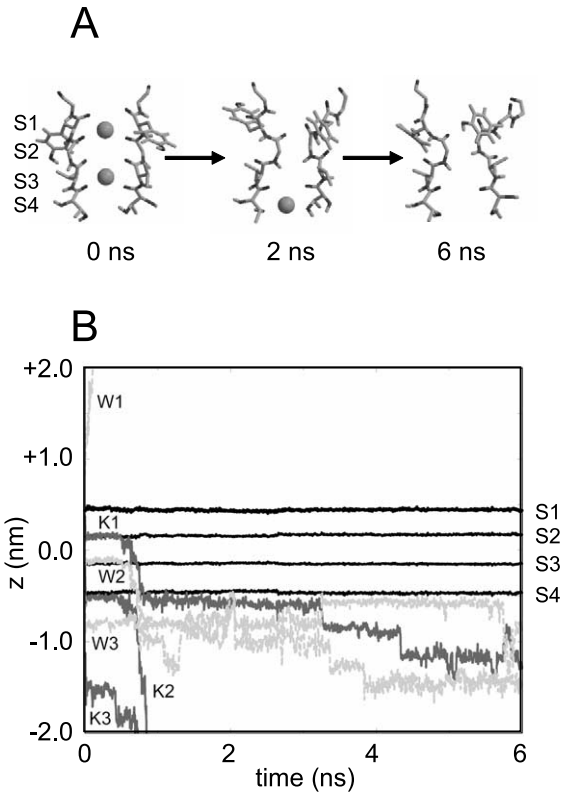

Fig. 6. A: Snapshots of the selectivity filter at the start ($t=0$), midway ($t=2$ ns) and at the end ($t=6$ ns) of the model B simulation. B: Trajectories, projected onto the pore axis, of the K^+ ions (dark grey lines) and water molecules (pale grey lines) initially within the filter. The centres of the four binding sites (S1–S4) are indicated by the horizontal black lines.

Kir6.2 which have altered conductance properties relative to the wild-type Kir6.2 channels [24]. Physiological studies of potassium channels suggest that K^+ ions may play a role in maintaining the structural integrity of the selectivity filter [48,49]. Thus, it seems that the filter of GluR0 behaves in a similar K^+-dependent fashion to that of K channels.

The movements of the two K^+ ions in the filter and the third K^+ ion in the cavity were analysed via calculating the z (i.e. pore axis) co-ordinate trajectories of the K^+ ions as a function of time (Fig. 6B). This revealed that early on in the simulation the K^+ ions in the filter and intervening water molecules moved in a concerted manner similar to that observed in simulations of KcsA [42,43,50–52] and of a Kir6.2 model [23,53]. Thus, the simulation starts with K1 at site S1 and K2 at site S3. Within the first ~0.9 ns they undergo a concerted translocation to S2 and S4 respectively. After a further ~0.5 ns K1 moves to S3, and then to S4, whilst K2 enters the cavity. K3 exits the cavity via the extracellular mouth (at ~0.7 ns) and K2 also subsequently exits at ~0.9 ns. K1 remains at site S4 until ~3.3 ns, at which time it also enters the cavity. This is correlated with a distortion of the filter geometry as it now does not hold any K^+ ions.

A similar behaviour has been seen in simulations of KcsA [40,42,44] and of a model of a mutant of Kir6.2 with altered conductance properties [24]. In the KcsA simulations once both of the ions have exited the filter it undergoes a substantial distortion so as to considerably narrow the central section of the filter. The distortion yields a filter conformation reminiscent of that observed in crystals of KcsA prepared in the presence of low K^+ ion concentrations [18]. It remains uncertain whether such changes in the conformation of the filter are responsible for 'fast gating' of K channels and GluR0 or whether they are part of the inherent flexibility required for rapid ion permeation through the filter.

Between ~0.8 ns and 3.3 ns, K1 interacts primarily with the carbonyl oxygens of T208 at site S4. Distance measurements reveal the average distance between K1 and the carbonyl oxygens to be ~0.26 nm, which corresponds to a close interaction [54]. A similarly close interaction is formed between K1 and the side chain (Oγ) of T208 from ~0.8 ns to ~4.3 ns. At ~3.3 ns, K1 and W2 (the water molecule initially in between K1 and K2) are seen to exchange positions along the pore axis. Closer inspection reveals that prior to the exchange, there appears to be 'competition' for binding to the carbonyl oxygens of site S4. The distance between these carbonyl oxygens and W2 decreases, and K1 is seen to be interacting primarily with the cavity waters. From this stage onwards until the end of the simulation, the interaction between K1 and the cavity waters steadily increases. This is seen from the decreasing distance between K1 and the oxygen atoms of the water molecules in the cavity (~0.3 nm on average) and the increased number of waters found in close proximity to K1.

Analysis of the motion of the ion K3 initially in the cavity reveals that it traverses the cavity, towards the extracellular mouth, in a step-wise fashion before exiting at ~0.7 ns. The pore radius profile in the region corresponding to residues C-terminal to A232 in M2 of GluR0 (corresponding to the hinge-bending G99 of KcsA) shows significant fluctuations associated with ion exit. Thus, some form of hinge-bending of M2 may occur in GluR0, although it is less clear-cut than the hinge-bending at G99 that is proposed to underlie gating of KcsA [39].

4. Conclusions

The results presented above support the contention that GluR0 has a structure similar to the K channel KcsA. In particular, the conformational stability of a model of the TM domain of GluR0 in simulations is the same as that of the TM domain of KcsA in comparable simulations. Comparison of two closely related models favours one in which the four residue insertion in the GluR0 sequence relative to KcsA is placed in the M1/P inter-helix loop, rather than in the P helix per se. Furthermore, the tetramer seems to be stabilised by inter-subunit salt bridges similar to those seen in KcsA. Concerted translocation of K^+ ions and water molecules along the filter is observed and, as with KcsA, the filter distorts to a 'fast closure' conformation in the absence of K^+ ions.

Of course, the model presented is only for the TM domain. Given that the structure of the glutamate-binding domain of GluR0 has been determined by crystallography, it may be possible to combine the two to come up with a model of the intact GluR0 molecule. This is not without its difficulties as the loop of peptide 'missing' between the GluR0 TM domain model and the ligand-binding domain structure is sufficiently long that it is not possible to model its conformation

with any certainty. Thus we cannot as yet comment directly on how the gating mechanism at the pore level is coupled to conformational changes in the ligand-binding domain. It remains a possibility that a more complex gating mechanism than that envisioned here operates. For example, ligand binding may induced M2 helix movement to open the hydrophobic gate and the resultant M2 helix movement and/or ion movement through the channel may lead to a change in the (time-averaged) filter structure that would correspond to a second ('fast') gate at the opposite end of the channel.

It should also be remembered that we remain uncertain as to the orientation of GluR0 in *bacterial* cell membranes. It remains a (formal) possibility that rather than being a receptor for extracellular glutamate, GluR0 functions as a K channel gated by intracellular glutamate. A possible extension of the TM domain would be to include the immediate pre-M1 sequence. Spectroscopic studies on KcsA [55] and the recent X-ray structure of KirBac [56] both reveal pre-M1 helices that lie approximately parallel to the bilayer. Interestingly, the pre-M1 region of GluR0 has a short region that could form an amphipathic α-helix and so might be expected to adopt a similar, bilayer-surface orientation to pre-M1 I KcsA and KirBac.

It is less certain that the current methodology could be readily extended to mammalian GluRs. In particular, mammalian GluRs do not contain a canonical TVGYG selectivity filter motif. For example, in GluR2 the corresponding motif is QQGCD. Given this difference, it is rather more difficult to model the TM domain of GluR2 to obtain a model stable in simulations (Arinaminpathy and Sansom, unpublished results). Furthermore, a complete model of the GluR2 TM domain would also require inclusion of additional helix per subunit, for which no structural template exists. However, none of these problems is insurmountable.

Acknowledgements: Many thanks to all of our colleagues for their encouragement and advice. Research in M.S.P.S.'s laboratory is funded by grants from the BBSRC, EPSRC, MRC and the Wellcome Trust. Our thanks to the Oxford Supercomputer Centre for access to facilities.

References

[1] Hille, B. (2001) Ionic Channels of Excitable Membranes, Sinauer Associates, Sunderland, MA.
[2] Egebjerg, J. and Jensen, H.S. (2002) in: Glutamate and GABA Receptors and Transporters. Structure, Function and Pharmacology (Krogsgaard-Larsen, P., Ed.), pp. 41–55, Taylor and Francis, London.
[3] Armstrong, N., Sun, Y., Chen, G.-Q. and Gouaux, E. (1998) Nature 395, 913–917.
[4] Armstrong, N. and Gouaux, E. (2000) Neuron 28, 165–181.
[5] Kasper, C., Lunn, M.-L., Liljefors, T., Gouaux, E., Egebjerg, J. and Kastrup, J.S. (2002) FEBS Lett. 531, 173–178.
[6] Jin, R., Horning, M., Mayer, M.L. and Gouaux, E. (2002) Biochemistry 41, 15635–15643.
[7] Lunn, M.-L., Hogner, A., Stensbøl, T.B., Gouaux, E., Egebjerg, J. and Kastrup, J.S. (2003) J. Med. Chem. 46, 872–875.
[8] Hogner, A., Greenwood, J.R., Liljefors, T., Lunn, M.-L., Egebjerg, J., Larsen, I.K., Gouaux, E. and Kastrup, J.S. (2003) J. Med. Chem. 46, 214–221.
[9] Hogner, A., Kastrup, J.S., Jin, R., Liljefors, T., Mayer, M.L., Egebjerg, J., Larsen, I.K. and Gouaux, E. (2002) J. Mol. Biol. 322, 93–109.
[10] Sun, Y., Olson, R., Horning, M., Armstrong, N., Mayer, M.L. and Gouaux, E. (2002) Nature 417, 245–253.
[11] McFeeters, R.L. and Oswald, R.E. (2002) Biochemistry 41, 10472–10481.
[12] Mendieta, J., Ramirez, G. and Gago, F. (2001) Proteins Struct. Funct. Genet. 44, 460–469.
[13] Arinaminpathy, T., Sansom, M.S.P. and Biggin, P.C. (2002) Biophys. J. 82, 676–683.
[14] Kuner, T., Seeburg, P.H. and Guy, H.R. (2003) Trends Neurosci. 26, 27–32.
[15] Chen, G.Q., Cui, C.H., Mayer, M.L. and Gouaux, E. (1999) Nature 402, 817–821.
[16] Mayer, M.L., Olson, R. and Gouaux, E. (2001) J. Mol. Biol. 311, 815–836.
[17] Doyle, D.A., Cabral, J.M., Pfuetzner, R.A., Kuo, A., Gulbis, J.M., Cohen, S.L., Cahit, B.T. and MacKinnon, R. (1998) Science 280, 69–77.
[18] Zhou, Y., Morais-Cabral, J.H., Kaufman, A. and MacKinnon, R. (2001) Nature 414, 43–48.
[19] Sprengel, R., Aronoff, R., Volkner, M., Schmitt, B., Mosbach, R. and Kuner, T. (2001) Trends Pharmacol. Sci. 22, 7–10.
[20] Kuner, T., Beck, C., Sakmann, B. and Seeburg, P.H. (2001) J. Neurosci. 21, 4162–4172.
[21] Panchenko, V.A., Glasser, C.R. and Mayer, M.L. (2001) J. Gen. Physiol. 117, 345–359.
[22] Capener, C.E., Kim, H.J., Arinaminpathy, Y. and Sansom, M.S.P. (2002) Hum. Mol. Genet. 11, 2425–2433.
[23] Capener, C.E., Shrivastava, I.H., Ranatunga, K.M., Forrest, L.R., Smith, G.R. and Sansom, M.S.P. (2000) Biophys. J. 78, 2929–2942.
[24] Capener, C.E., Proks, P., Ashcroft, F.M. and Sansom, M.S.P. (2003) Biophys. J. 84, 2345–2356.
[25] Loussouarn, G., Makhina, E.N., Rose, T. and Nichols, C.G. (2000) J. Biol. Chem. 275, 1137–1144.
[26] Durell, S.R. and Guy, H.R. (2001) BioMed Cent. Evol. Biol. 1, 14.
[27] Sali, A. and Blundell, T.L. (1993) J. Mol. Biol. 234, 779–815.
[28] Sali, A. (1994) Protein Sci. 3, 1582–1596.
[29] Laskowski, R.A., Macarthur, M.W., Moss, D.S. and Thornton, J.M. (1993) J. Appl. Crystallogr. 26, 283–291.
[30] Adcock, C., Smith, G.R. and Sansom, M.S.P. (1998) Biophys. J. 75, 1211–1222.
[31] Davis, M.E., Madura, J.D., Luty, B.A. and McCammon, J.A. (1991) Comput. Phys. Commun. 62, 187–197.
[32] Berendsen, H.J.C., Postma, J.P.M., van Gunsteren, W.F. and Hermans, J. (1981) Intermolecular Forces, Reidel, Dordrecht.
[33] Berendsen, H.J.C., van der Spoel, D. and van Drunen, R. (1995) Comp. Phys. Commun. 95, 43–56.
[34] Hess, B., Bekker, H., Berendsen, H.J.C. and Fraaije, J.G.E.M. (1997) J. Comp. Chem. 18, 1463–1472.
[35] Berendsen, H.J.C., Postma, J.P.M., van Gunsteren, W.F., DiNola, A. and Haak, J.R. (1984) J. Chem. Phys. 81, 3684–3690.
[36] Kraulis, P.J. (1991) J. Appl. Crystallogr. 24, 946–950.
[37] Merritt, E.A. and Bacon, D.J. (1997) Methods Enzymol. 277, 505–524.
[38] Kabsch, W. and Sander, C. (1983) Biopolymers 22, 2577–2637.
[39] Jiang, Y., Lee, A., Chen, J., Cadene, M., Chait, B.T. and MacKinnon, R. (2002) Nature 417, 523–526.
[40] Holyoake, J., Domene, C., Bright, J.N. and Sansom, M.S.P. (2003) Eur. Biophys. J. (in press).
[41] Killian, J.A. and von Heijne, G. (2000) Trends Biochem. Sci. 25, 429–434.
[42] Shrivastava, I.H. and Sansom, M.S.P. (2000) Biophys. J. 78, 557–570.
[43] Shrivastava, I.H., Tieleman, D.P., Biggin, P.C. and Sansom, M.S.P. (2002) Biophys. J. 83, 633–645.
[44] Domene, C. and Sansom, M.S.P. (2003) Biophys. J. (in press), ms. 2002/018044.
[45] Perozo, E., Cortes, D.M. and Cuello, L.G. (1998) Nat. Struct. Biol. 5, 459–469.
[46] Kirsch, G.E., Pascual, J.M. and Shieh, C.C. (1995) Biophys. J. 68, 1804–1813.
[47] Pascual, J.M., Shieh, C.C., Kirsch, G.E. and Brown, A.M. (1995) Neuron 14, 1055–1063.
[48] Melishchuk, A., Loboda, A. and Armstrong, C.M. (1998) Biophys. J. 75, 1828–1835.

[49] Ogielska, E.M. and Aldrich, R.W. (1999) J. Gen. Physiol. 113, 347–358.
[50] Sansom, M.S.P., Shrivastava, I.H., Bright, J.N., Tate, J., Capener, C.E. and Biggin, P.C. (2002) Biochim. Biophys. Acta 1565, 294–307.
[51] Bernèche, S. and Roux, B. (2000) Biophys. J. 78, 2900–2917.
[52] Bernèche, S. and Roux, B. (2001) Nature 414, 73–77.
[53] Capener, C.E. and Sansom, M.S.P. (2002) J. Phys. Chem. B 106, 4543–4551.
[54] Tieleman, D.P., Biggin, P.C., Smith, G.R. and Sansom, M.S.P. (2001) Q. Rev. Biophys. 34, 473–561.
[55] Cortes, D.M., Cuello, L.G. and Perozo, E. (2001) J. Gen. Physiol. 117, 165–180.
[56] Kuo, A., Gulbis, J.M., Antcliff, J.F., Rahman, T., Lowe, E.D., Zimmer, J., Cuthbertson, J., Ashcroft, F.M., Ezaki, T. and Doyle, D.A. (2003) Science 330, 1921–1926.